Journal of Crystal Growth 101 (1990) 350–354
North-Holland

TUNNELING CURRENT CALCULATED FOR $Hg_{0.8}Cd_{0.2}Te$ DIODES

A. SCHENK, M. STAHL and H.-J. WÜNSCHE

Sektion Physik der Humboldt-Universität zu Berlin, Invalidenstrasse 110, DDR-1040 Berlin, German Dem. Rep.

The influence of the doping profile on the soft breakdown in $Hg_{0.8}Cd_{0.2}Te$ photodiodes is investigated theoretically. The abrupt, linear, n^+p^-p and n^+n^-p models are compared one with another using an improved formulae for the interband tunneling generation rate, valid for both strong and inhomogeneous fields. The stationary semiconductor device equations are solved numerically including degeneracy and KANE band structure. The $I-U$ characteristics of the various models are discussed for the different operating modes of the diode.

1. Introduction

In narrow gap diodes, a soft reverse breakdown can be caused by interband tunneling at comparatively low voltages. The breakdown characteristic depends on the profile of electrically active species, on temperature and on carrier lifetimes, which are related to the induced damage.

In this paper we investigate the $I-U$ characteristics of n^+p-HgCdTe photodiodes theoretically. First, the junction potential is calculated by numerically solving the stationary semiconductor device equations [1] for four different models of the doping profile. The potential shape then enters an improved formulae for the interband tunneling generation rate, which holds in the case of an essentially inhomogeneous field at small bias as well as in the strong field case of breakdown bias [2]. Besides the tunneling rate, Auger and Shockley–Hall–Read (SHR) recombination rates are taken into account in the numerical calculation of the total current. Finally we will discuss the proposed n^+p^-p and n^+n^-p junction models in HgCdTe diodes [3] with respect to carrier lifetimes and tunneling contributions to the R_0A product.

2. Theoretical method

The current density of the n^+p-HgCdTe photodiode is calculated solving the Van Roosbroeck system of semiconductor device equations [1], Poisson equation and continuity equations for electrons and holes, in one dimension:

$$\epsilon_0 \frac{\mathrm{d}}{\mathrm{d}x}\left(\epsilon \frac{\mathrm{d}}{\mathrm{d}x}\phi\right) = -e\left[p(x) - n(x) + N_D^+(x) - N_A^-(x)\right], \quad (1)$$

$$\frac{\mathrm{d}}{\mathrm{d}x} j_p = -\frac{\mathrm{d}}{\mathrm{d}x} j_n = eR, \quad (2)$$

where ϕ is the electrostatic potential and R the net recombination rate. The above equations use ϕ, n and p as basic quantities. The current densities of electrons and holes are proportional to the gradients of the quasi-Fermi potentials η_n and η_p:

$$j_n = e\mu_n n \frac{\mathrm{d}}{\mathrm{d}x}\eta_n, \quad (3a)$$

$$j_p = e\mu_p p \frac{\mathrm{d}}{\mathrm{d}x}\eta_p. \quad (3b)$$

η_n and η_p are determined by ϕ, n and p according to

$$n = N_c J_{1/2}\left(\frac{e\eta_n - E_c + e\phi}{kT}, \gamma\right), \quad (4a)$$

$$p = N_{hh} J_{1/2}\left(\frac{E_v - e\eta_p - e\phi}{kT}, 0\right), \quad (4b)$$

where $N_{c,hh}$ denote the effective densities of states of electrons and heavy holes, $E_{c,v}$ the band edge energies and γ the Kane parameter $\gamma = kT/E_g$,

0022-0248/90/$03.50

respectively. $J_{1/2}$ substitutes the common Fermi integral by

$$J_{1/2}(\zeta, \gamma) = \frac{2}{\sqrt{\pi}} \int_0^\infty \mathrm{d}x \frac{[x(1+\gamma x)]^{1/2}(1+2\gamma x)}{1+\exp(x-\zeta)}. \tag{5}$$

Kane band structure and degeneracy have been incorporated into the device simulation packages "MEDEA ID©" and "TOSCA©". The structure is modeled as 20 microns layer $Hg_{0.8}Cd_{0.2}Te$ on CdTe substrate with front- and backside ohmic contacts. Furthermore, interband tunneling in the space charge layer is considered to be responsible for the reverse breakdown. In contrast to Auger and SHR recombination, the tunneling generation is nonlocal due to the inhomogeneous field in the depletion region. This inhomogeneity is increasingly important for low bias operation. Standard WKB calculations of the tunneling rate would suit this case, but they fail in the breakdown region of highly doped, abrupt junctions. A theory which combines both the WKB approximation, valid for inhomogeneous but low fields, and the EMA treatment, valid for large but homogeneous fields, has been outlined in ref. [2]. The integration of the tunneling rate over the space charge layer has been converted into an integration over the allowed energy interval there. As a result, the tunneling current density is given by

$$j_t = -e \int G_t(E) \left[f_v(E) - f_c(E) \right] \mathrm{d}E. \tag{6}$$

$G_t(E)$ denotes the energetic tunneling rate:

$$G_t(E) = \frac{3|eF(x_0)|^3 m_v m_c S_{red}(x_0)}{128\pi m_{red}^2 E_g^3 (2m_{red}E_g)^{1/3}} \times \theta(E_v - E - e\phi_v)\, \theta(E - E_c + e\phi_c)\, \Lambda(x_0), \tag{7}$$

with

$$\Lambda(x_0) = 8\pi\, \zeta(x_0) \left\{ \mathrm{Ai}^2[\zeta(x_0)] - \zeta(x_0)\, \mathrm{Ai}'^2[\zeta(x_0)] \right\}, \tag{8}$$

$$\zeta(x_0) = \left[\tfrac{3}{2} |S_c(x_0) - S_v(x_0)| \right]^{2/3}. \tag{9}$$

In (9), the actions $S_\nu(x_0)$ are defined by

$$S_\nu(x_0) = \frac{\sqrt{2m_\nu}}{\hbar} \int_{x_\nu}^{x_0} \mathrm{d}x' \sqrt{e|\phi(x') - \phi(x_\nu)|}, \tag{10}$$

where x_ν are the turning points, and x_0 is solution of the implicit relation

$$(m_c + m_v)\, \phi(x_0) = m_v \phi(x_v) = m_c \phi(x_c). \tag{11}$$

The notation is as follows: F is the electric field strength, m_c and m_v are the effective band masses of electrons and light holes, respectively, m_{red} is the reduced effective mass, S_{red} is the reduced action, f_ν is the Fermi function, θ is a step function, ϕ_c and ϕ_v are the boundary values of the electrostatic potential, and Ai and Ai′ are Airy functions.

Eqs. (10) and (11) are solved inserting for ϕ the numerical result of (1) to (5). The computed tunneling current density then is added to the result of (2). Although this procedure is not completely self-consistent, because the feedback of the tunneling current on the electrostatic potential is not properly taken into account, the error in the breakdown characteristic should be small. This is due to the fact that the number of generated carriers is always much smaller than the doping concentration.

3. Numerical results

Besides the common abrupt and linear junctions, we have investigated n^+p^-p- and n^+n^-p-type junction electrical profiles, discussed by Bubulac et al. [3]. Those profiles are thought to be the result of limited diffusion of displaced Hg in conjunction with a p-type or an n-type impurity background (residual or intentionally impurity doped). The input profiles for our numerical calculation are shown in fig. 1. The impurity background concentration has been given the value of $1 \times 10^{15}\,\mathrm{cm}^{-3}$, but it has been varied in the case of the n^+n^-p-type junction to determine its influence on the breakdown position. The "linear"

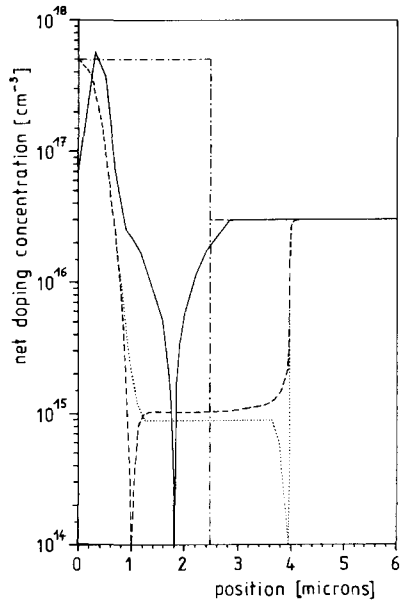

Fig. 1. Net doping profiles of abrupt (dash-dotted line), linear (full line), n^+p^-p (dashed line) and n^+n^-p junction (dotted line).

profile is exactly linear only from 1 to 3 μm, but this region covers the whole depletion layer.

I–U characteristics for the diffusion limited diode are shown in fig. 2. The Auger coefficients for electrons and holes were calculated from an

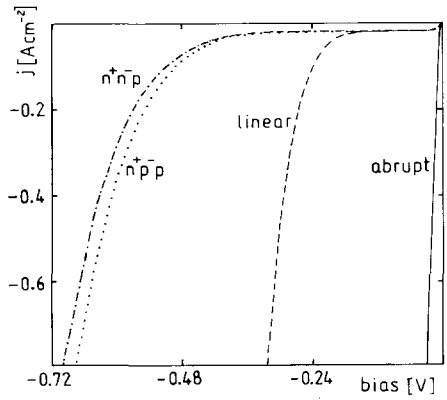

Fig. 2. *I–U* characteristics of abrupt (full line), linear (dashed line), n^+p^-p (dotted line) and n^+n-p junction (dash-dotted line). Parameters: $T = 77$ K, $\mu_n = 8\times10^4$ cm^2/V·s, $\mu_p = 7\times10^2$cm^2/V·s, $\tau_{SHR} = 1\times10^{-4}$ s, $m_c = 0.007m_0$, $m_{hh} = 0.44m_0$, ϵ after ref. [5], E_{gap} after ref. [6]. For Auger coefficients, see text.

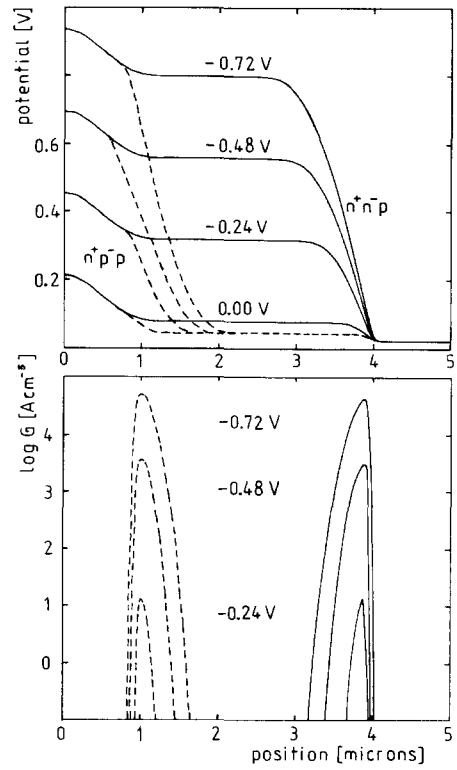

Fig. 3. Potential shape and interband tunneling rate of the n^+p^-p and n^+n^-p junction diodes.

expression in ref. [4] to be $G_{Ae} = 9.216\times10^{-25}$ cm^6 s^{-1} and $G_{Ah} = 5.096\times10^{-25}$ cm^6 s^{-1} at 77 K. In the case of the abrupt junction model no saturation of the reverse current is observed up to

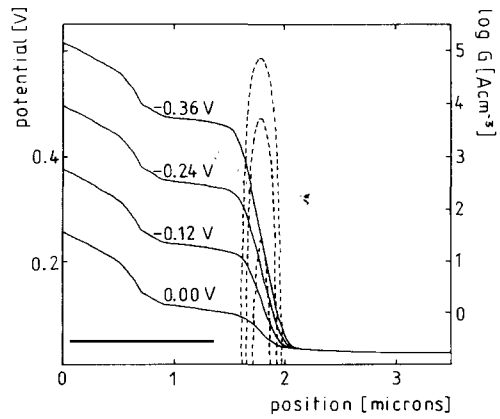

Fig. 4. Potential shape and interband tunneling rate of the linear junction diode.

-1×10^{-2} V bias. In all other cases the saturation current density reaches a value of -1.8×10^{-2} A cm^{-2}, but the breakdown characteristics differ remarkably. The linearly graded n^+p junction (profile gradient: 2.81×10^{16} cm$^{-3}/\mu$m) exhibits a soft breakdown starting at about -180 mV, whereas the n^+n^-p and n^+p^-p structures are very similar in their breakdown position at about -450 mV as well as in their form of the breakdown, which is smoother than in the case of the linear junction profile.

Figs. 3 and 4 show a detailed analysis of the electrostatic potentials and the tunneling rates of the n^+p^-p, n^+n^-p and linear junction model structures, respectively, using the applied bias as parameter. In order to visualize the interband tunneling rate as function of the x coordinate, it has been transformed by the relation

$$G(x) = G(x_0(E)) = G(E(x))\, \mathrm{d}E(x)/\mathrm{d}x$$

for $x = x_0(E)$, and the Fermi occupation functions have been included in the definition of $G(x)$. Asymmetrical junctions are reflected by asymmetrical distributions of the tunneling rate.

If we look at the influence of the n-type impurity background concentration on the breakdown threshold of the n^+n^-p junction model diode, we find that the decrease of the n^- level shifts the breakdown to larger reverse voltages and flats the curves. This is demonstrated in fig. 5. For given p-side acceptor concentrations, the calculated

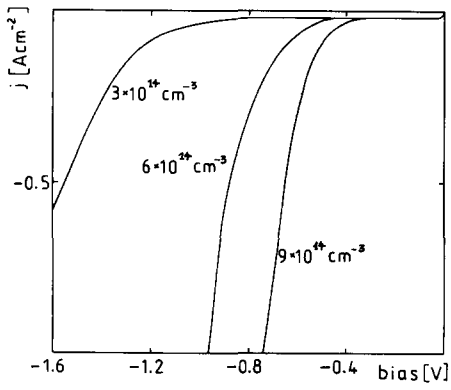

Fig. 5. I–U characteristics for different levels of the background impurity concentration of the n^+n^-p junction diode (other parameters unchanged).

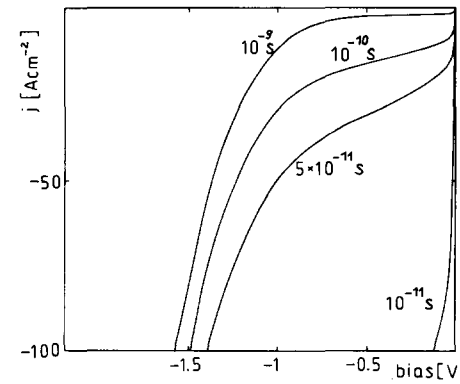

Fig. 6. I–U characteristics of the n^+p^-p junction model diode for decreasing SHR lifetimes (other parameters unchanged).

breakdown threshold can serve as an estimate of the n-type impurity background level.

The above results are related to diodes of high quality, where the material is essentially damage free. The deep lying n^+n^-p junction could be well described by them. However, an n^+p^-p junction in the near surface layer with high defect concentration might result in a low quality, generation-recombination limited diode. We studied this case varying the SHR lifetime. The corresponding I–U characteristics are shown in fig. 6. For $\tau_{SHR} < 1 \times 10^{-10}$ s, the diode operates in the generation-recombination mode with increasing values and gradients of the current density. The superimposed tunneling breakdown becomes more and more undistinguishable from the recombination current.

Finally, we found that in no case the R_0A product is influenced by the interband tunneling at 77 K. In the case of n^+n^-p and n^+p^-p junction diodes this remains true down to temperatures where the holes freeze out.

4. Summary

The interband tunneling generation rate has been included in the numerical solvation of the system of stationary semiconductor transport equations. Breakdown characteristics of a $Hg_{0.8}Cd_{0.2}Te$ photodiode were investigated with respect to various possible doping profiles. No breakdown

before -0.4 V is expected in the case of a high quality, diffusion limited n^+n^-p junction diode with a background impurity level of about 1×10^{15} cm^{-3}. A further decrease of this level results in a remarkable improvement of such diodes. One can estimate the background concentration from the calculated breakdown. Low quality diodes with a large recombination current density have larger breakdown voltages too, but for very small SHR lifetimes the tunneling branch is no longer emphasized in the $I-U$ characteristic.

Acknowledgement

The authors are indebted to Professor H. Gajewski and Dr. J. Fuhrmann (Institute of Mathematics, Academy of Sciences, Berlin, GDR) for their help in modifying the programs MEDEA ID and TOSCA, respectively. The unconstrained utilization of these programs is gratefully acknowledged.

References

[1] W. Van Roosbroeck, Bell Syst. Tech. J. 29 (1950) 560.
[2] A. Schenk, M. Stahl and H.-J. Wünsche, Phys. Status Solidi (b) 154 (1989) 815.
[3] L.O. Bubulac, W.E. Tennant, D.S. Lo, D.D. Edwall, J.C. Robinson, J.S. Chen and G. Bostrup, J. Vacuum Sci. Technol. A 5(5) (1987) 3166.
[4] C.J. Summers and B. Darling, J. Appl. Phys. 59 (1986) 2457.
[5] R. Dornhaus and G. Nimtz, Solid State Phys. 78 (1976) 1.
[6] E. Finkman and S.E. Schacham, J. Appl. Phys. 56 (1984) 2896.